Electrochemical Atomic-Force Microscopy Using a Tip-Attached Redox Mediator. Proof-of-Concept and Perspectives for Functional Probing of Nanosystems

Agnès Anne, Christophe Demaille,* and Cédric Goyer

Laboratoire d'Electrochimie Moléculaire, Unité Mixte de Recherche Université - CNRS No. 7591, Université Paris Diderot (Paris 7), 15 rue Jean-Antoine de Baïf, 75205 Paris Cedex 13, France

ABSTRACT This paper presents the first steps toward the development of a new type of high-resolution AFM-SECM microscopy which relies on the use of tip-attached redox-labeled polymer chains as mediators to probe the local electrochemical reactivity of a planar substrate at the nanoscale. Submicrometer-sized combined gold AFM-SECM probes were functionalized by linear, nanometer-sized, flexible, PEG_{3400} chains bearing a ferrocene (Fc) redox label at their free end. Analysis of the force and current approach curves recorded when such Fc-PEGylated probes (tips) were approached to a bare gold substrate allowed the presence of the Fc-PEG chains at the very tip end of the combined probes to be specifically demonstrated. It also allowed the chain coverage, configuration, and dynamics to be determined. When the Fc-PEGylated probe is positioned some ~5 nm above the substrate, only a few hundred chains are actually electrochemically contacting the surface, thus reducing the size of the tip—substrate interaction area to 20—40 nm. Most importantly, we have shown that the tip-borne PEG chains are flexible enough to allow their Fc heads to efficiently "sense" locally the electrochemical reactivity of the substrate, thus validating the working principle of the new AFM-SECM microscopy we propose. This innovative microscopy, we label Tarm (for tip-attached redox mediator)/AFM-SECM, should be particularly suitable for probing the activity of slowly functioning nanometer-sized active sites on surfaces, such as individual enzyme molecules, because it is, by design, free of the diffusional constraints which hamper the characterization of such nanosystems by classical SECM.

KEYWORDS: electrochemical microscopy · SECM · electrochemical atomic-force microscopy AFM/SECM · tip-attached redox mediator/electrochemical atomic-force microscopy · Tarm/AFM-SECM · redox-functionalized AFM tips

Among the "near-field" microscopy techniques, scanning electrochemical microscopy (SECM) has the unique ability to probe the local reactivity of surfaces.[1−3] In a classical SECM configuration, a microelectrode (tip), of a size in the micro- to the nanometer range, is approached *in situ* toward a substrate immersed in an electrolyte solution containing a soluble redox mediator. SECM can be operated in either the so-called feedback or collection modes.[1] In SECM feedback mode, the microelectrode is biased so as to oxidize or reduce the redox mediator, thus generating its "active" redox form, which then diffuses toward the electrochemically reactive substrate surface. As a result, the initial redox form of the mediator is regenerated and is fed back to the tip, thus increasing the tip current. The dependence of the tip current on the tip−substrate separation can then be used to characterize the kinetics of the electrochemical reaction taking place at the substrate surface. Alternatively, the SECM can also be operated in the collection mode where an electroactive product is generated at the substrate surface and collected at the tip.[1] In both of its operating modes, the SECM can be used to construct tip-current images, by scanning the microelectrode over the substrate surface, thus allowing the distribution of electroactive sites present over the substrate surface to be spatially resolved and their individual reactivity probed.[4−7] The lateral resolution of SECM is ultimately governed by the size of the microelectrode and has long remained in the micrometer range. Recently, a large amount of work has been devoted to increase the resolution of SECM toward the nanometer range by using ever smaller microelectrodes, of sizes as small as a few tens of nanometers.[8−11] In order to control the approach of these tips from surfaces, it is most useful to couple SECM with other local probe techniques. Coupling of SECM with atomic-force microscopy (AFM) has been notably reported,[12−22] and the fabrication of combined AFM-SECM probes bearing nanometer-sized microelectrode tips has also been described.[19,20] However, the fabrication of nanoelectrodes usable as

*Address correspondence to demaille@univ-paris-diderot.fr.

Received for review November 17, 2008 and accepted March 05, 2009.

Published online March 12, 2009.
10.1021/nn8007788 CCC: $40.75

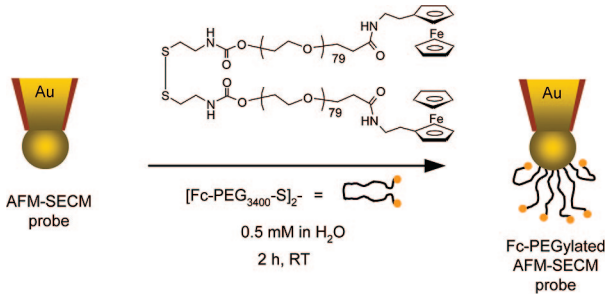

Figure 1. Functionalization of an AFM-SECM combined probe by the home-prepared Fc-PEG$_{3400}$−disulfide molecule, yielding a Fc-PEGylated AFM-SECM probe.

SECM probes remains a difficult task, while actual nanometer-sized combined AFM-SECM probes can only be fabricated using sophisticated microfabrication techniques hardly available to experimentalists.[19,20,22]

Moreover, beyond technical constraints, probing the reactivity of a surface at the nanoscale by SECM is hampered by a fundamental limitation: SECM can only probe surface reactivity if the turnover of the surface reaction is fast enough with respect to the diffusion rate of the soluble redox mediator.[4,23,24] The diffusion rate can be defined as the time it takes for the mediator to diffuse on a distance corresponding to the probe size. Therefore, increasing the lateral resolution of SECM by simply decreasing the microelectrode size leads to the following paradox: resolving small reactive sites on a surface requests small probes, but decreasing the probe size increases the rate of diffusion up to the point where comparatively "slow"-reacting sites become undetectable by SECM.[3] This problem is particularly acute for the detection and functional probing of surface-immobilized individual enzyme molecules,[25,26] which are intrinsically "slowly" functioning nano-objects.[27]

In that context, we are presenting here the first steps of a project aiming at developing an electrochemical atomic-force microscopy with the SECM mediator attached to the probe, we label Tarm (for tip-attached redox mediator)/AFM-SECM. This new type of SECM microscopy, being free of the above limitations, should, in principle, allow the reactivity of nanometer-sized surface sites to be probed independently of their turnover rate. In the proposed configuration, flexible, hydrophilic, biocompatible, polyethylene glycol (PEG)$_{3400}$ chains, bearing a redox ferrocene (Fc) moiety at their free end, are attached by their other extremity to the gold surface of combined AFM-SECM probes. The AFM-SECM configuration will allow the tip-borne Fc-PEG chains to be brought in the vicinity of individual reactive sites. Being indefinitely confined in the vicinity of the active sites, the Fc heads will then be given enough time to react with them and to be exhaustively collected back by the tip.

An original aspect of the proposed configuration is that the lateral resolution of this new type of electrochemical microscopy will be governed by the nanometer dimension of the Fc-PEG "molecular probes" and will consequently be much less tip-size-dependent than in the case of classical SECM.[1]

RESULTS AND DISCUSSION

Choice of the "Molecular Probes" To Be Attached to the Tip for Tarm/AFM-SECM Microscopy. AFM tips modified with redox groups have been previously reported.[28] They were fabricated with the aim of controlling the tip−surface adhesion and for lithographic applications but in a context completely remote from SECM.[29] In the present work, linear Fc-PEG$_{3400}$ disulfide molecules made of poly(ethylene glycol) chains of 3400 molecular weight and bearing a redox ferrocene moiety (Fc) head at each extremity were custom-synthesized to be used as molecular probes for Tarm/AFM-SECM microscopy. Fc-PEG$_{3400}$ chains were specifically chosen since we demonstrated that, when grafted onto a gold planar surface *via* a sulfur−gold linkage, Fc-PEG$_{3400}$ chains form robust layers.[30,31] We have also shown that, when these layers are probed by an incoming bare AFM-SECM tip, the chains display the required hydrophilicity and flexibility for their Fc heads to efficiently shuttle electrons from the substrate to the tip across nanometer-sized tip−substrate gaps.[17,18] Fc-PEG chains also exhibited the necessary biocompatibility to convey electrons within integrated enzymatic systems consisting of organized multilayers of glucose oxidase assembled onto an electrode.[32,33] In these systems the PEG-borne Fc heads were able to reach the prosthetic group of the enzyme, albeit buried within the enzyme's catalytic pocket, where they served as efficient cofactors. This provides a clear illustration of the ability of Fc-PEG chains to explore confined nanospaces.

Terminal Attachment of the Fc-PEG Chains to the Spherical Apex of the Combined AFM-SECM Probe. The homemade AFM-SECM probes (tips) used here were described previously.[16] They consist in a bent gold microwire, flattened to act as a flexible cantilever, and bearing a very smooth spherical tip of submicrometer dimension. The probe is entirely insulated by deposition of electrophoretic paint, glued onto a standard AFM silicon chip, and its spherical tip end is selectively exposed in order to act as a current-sensing microelectrode (see Experimental Methods).

Functionalization of the gold spherical microelectrode was carried out by immersing the extremity of a combined probe into a drop of an aqueous solution containing ~0.5 mM of the Fc-PEG−disulfide molecule for ~2 h. This resulted in the direct covalent end-grafting of the Fc-PEG chains to the surface of the spherical tip end *via* a stable gold−"sulfur" bond, as sketched in Figure 1.

At this stage, it is required that the resulting Fc-PEGylated probe is characterized and, in particular, that the Fc-PEG chain coverage of the probe is determined. To do so, one could, in principle, record a cyclic

voltammogram at the Fc-PEGylated probe immersed in a supporting electrolyte solution. Integration of the faradaic current signal, resulting from the electrochemical detection of the Fc heads, would then yield access to the chain coverage. However, we observed that the cyclic voltammograms recorded at Fc-PEGylated probes only show a large capacitive component. This is not surprising since one has to bear in mind that only the very apex of the spherical AFM/SECM probe, of ~500 nm radius, is exposed to the solution. Therefore, the number of Fc-PEG molecules borne by the tip is very low and, consequently, gives rise to an intrinsically very low current in CV. Moreover, to this faradaic signal is superimposed a much larger current corresponding to the charging of the electrochemical capacity of the probe (~100 pf). This problem makes it difficult to measure the coverage of redox monolayer functionalized microelectrodes by cyclic voltammetry, as previously reported.[11]

We therefore turned to approach curve analysis for the characterization of the tip-borne Fc-PEG layer. This method has the inherent merit of allowing the Fc-PEG chains immobilized at the very apex of the probe (*i.e.*, the only ones ultimately "sensing" the substrate) to be selectivity addressed.

Characterization of the Fc-PEGylated Probes by Contact Mode AFM-SECM. ***Determining the Chain Coverage, Configuration, and Dynamics from Approach Curves.*** A Fc-PEGylated AFM-SECM combined probe (tip) was mounted onto the AFM microscope and approached toward a flat planar template-stripped gold substrate in a 1 M $NaClO_4$ containing aqueous electrolyte solution. The Fc-PEGylated tip and the bare substrate were respectively biased at potentials largely positive (E_{tip} = +0.30 V/SCE) and largely negative (E_{sub} = −0.10 V/SCE) with respect to the standard potential of the ferrocene head ($E°$ = +0.15 V/SCE).[17] Recording the tip deflection and the tip current simultaneously, while the tip was approached toward the substrate, allowed AFM-SECM approach curves to be constructed. Figure 2a,b shows representative, simultaneously acquired, force and current approach curves (solid blue lines). Figure 2a shows the force approach curve, in which the force experienced by the Fc-PEGylated tip, *F*, is plotted as a function of the tip−substrate distance *d*. Figure 2b shows the current approach curve, where the current circulating through the tip is plotted as a function of *d*. These approach curves were derived from the raw tip deflection and tip current *versus* piezo elongation data, proceeding as previously reported and as detailed in Experimental Methods.

Force Curve Analysis. As seen in Figure 2a when the tip−substrate distance decreases below ~10 nm, and down to $d \sim 7$ nm, the Fc-PEGylated probe senses a weak attractive force (*i.e.*, the tip is deflected downward). For $d < 7$ nm, the tip experiences a repulsive force, which increases steadily in magnitude as *d* is decreased. The recorded force curve is strikingly different

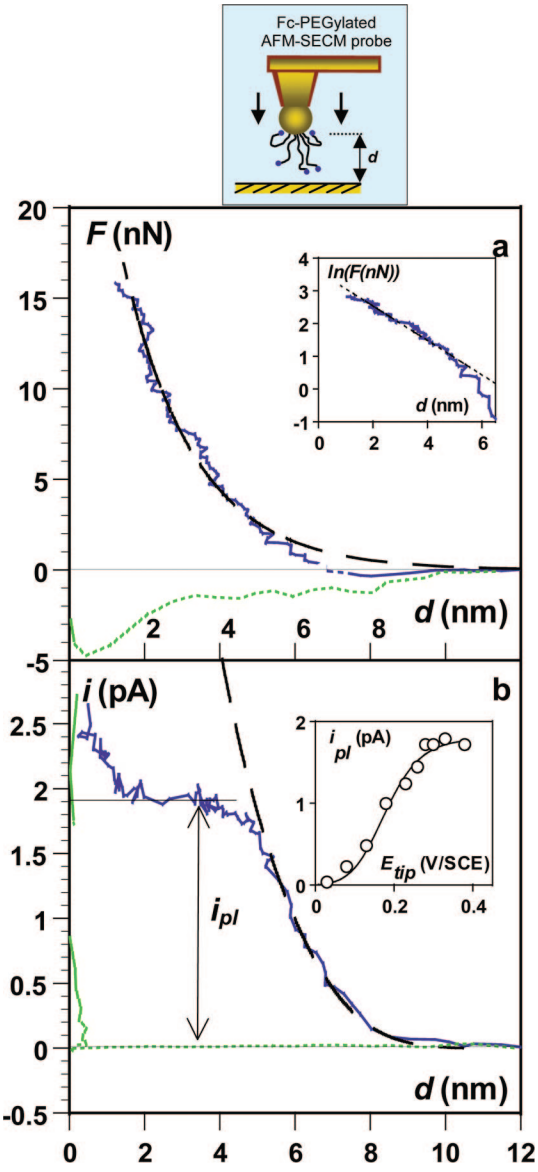

Figure 2. Characterization of a Fc-PEGylated probe by contact mode AFM-SECM. Force (a) and current (b) AFM-SECM approach curves recorded simultaneously upon approaching an AFM-SECM probe bearing a layer of end-grafted Fc-PEG_{3400} chains (Fc-PEGylated probe, blue solid line) or a bare AFM-SECM probe (green dashed line) from a bare gold surface. (a) Force sensed by the tip, *F*, is calculated from the tip deflection and plotted as a function of the tip−substrate separation *d*. The inset shows the corresponding ln(*F*) *vs d* plot and its best-fit linear regression calculated for the 2−5 nm region (dotted line), yielding the parameters F_0 = 35 nN and R_g = 1.9 nm (see text). The dashed curve is the theoretical force curve for the compression of a layer of polymer chains in a mushroom configuration calculated using these F_0 and R_g values. (b) Experimental current approach curve is fitted by the theoretical elastic bounded diffusion SECM positive feedback curve using, as a single adjustable parameter, the value of the characteristic current of i_0 = 80 pA. The inset shows the variation of i_{pl}, the intensity of the current of the plateau observed in the current approach curve for $d \sim 4$ nm, as a function of the tip potential E_{tip} (white dots). The line passing through the white dots is only a guide to the eye. The substrate potential E_{sub} was held at −0.1 V/SCE, the tip potential was E_{tip} = +0.3 V/SCE unless otherwise mentioned; 1 M $NaClO_4$ supporting aqueous electrolyte.

from the one recorded with a bare tip approaching a bare gold surface (dotted green curve). In this later case, the force is purely attractive and the approach curve displays a characteristic minimum corresponding to the point where the tip jumps into contact with the gold substrate. The observed "rounded" shape of the force approach curve recorded using the Fc-PEGylated probe is at the opposite highly reminiscent of the one we described previously in the case of a bare AFM-SECM gold tip approaching a gold substrate bearing a molecular monolayer of Fc-PEG_{3400} chains.[17,18] This result is a first indication of the presence of a layer of end-grafted Fc-PEG chains on the apex of the spherical gold tip. Within this layer, the Fc-PEG chains can adopt two different conformations depending on the proximity of neighboring chains (*i.e.*, on the grafting density). At low grafting densities, the chains are sufficiently far apart to form non-interacting hemispherical blobs, referred to as mushrooms, of a size similar to their free Flory radius in solution, R_F. At high grafting densities, the interchain distance is lower than R_F and the chains elongate toward the solution to minimize lateral interactions, forming a so-called polymer brush. The Flory radius of the PEG chains in water, a good solvent for PEG, is given by $R_F = aN^{3/5}$, N being the number of monomers of the chain and a the statistical monomer size.[34,35] Since here $N \sim 79$ and $a = 0.35$ nm,[36,37] the characteristic size of the coiled chains is $R_F \sim 5$ nm. Therefore, the Fc-PEG chains are expected to adopt a brush conformation for coverages such that $\Gamma \gg 1/(NR_F^2) = 0.7 \times 10^{-11}$ mol/cm^2.

As detailed below, and as reported for other polymer functionalized AFM probes,[38] analysis of the force approach curve can be used to gain insights into the conformation of the Fc-PEG layer end-grafted onto the apex of the AFM-SECM probes. It seems relevant to start by comparing the compression behavior we report here to the one theoretically predicted for the compression, by a spherical tip, of a layer of linear polymer chains end-grafted to a *planar* surface.

The compression of polymer mushrooms and brushes results, in the moderate compression regime, in a force exponentially decaying with the confinement distance and given by $F = F_0 \exp[-d/d_0]$.[39] The expressions of the pre-exponential term F_0 and of the decay length d_0 depend on the density of the end-grafted layer: For mushroom layers, $F_0 = 72\pi R_{tip}\Gamma RT$ and $d_0 = R_g$, where R_{tip} is the tip radius, Γ the chain coverage, and $R_g = R_F/\sqrt{6}$ is the radius of gyration of the coiled chain.[39,40] For brush-like layers, $F_0 = 100hk_BTR_{tip}(\Gamma N)^{3/2}$, $d_0 = h/2\pi$, with h the brush thickness.[39,41] As evidenced by the ln(F) *vs* d plot presented in the inset of Figure 2, and despite the different geometry involved, we also observed an exponentially decaying force curve when a Fc-PEGylated probe was approached toward a bare gold surface. More quantitatively, linear regression analysis of the ln(F) *vs* d variation, in the $d = 2-5$ nm region, yields best-fit values of $d_0 = (1.9 \pm 0.5)$ nm and of $F_0 = (35 \pm 5)$ nN. Taking for R_{tip} the measured tip radius of ~500 nm, the brush scenario yields $h = 12$ nm and $\Gamma = (1.1 \pm 0.1) \times 10^{-11}$ mol/cm^2, which would indicate a strong elongation of the chains ($h > R_F$), for a paradoxically low surface coverage, not fulfilling the $\Gamma \gg 1/(NR_F^2)$ "brush" condition. The mushroom scenario yields a value of $R_g = (1.9 \pm 0.5)$ nm and a chain coverage of $\Gamma = (1.2 \pm 0.2) \times 10^{-11}$ mol/cm^2. This experimental R_g value is close tothe expected value of $R_g = R_F/\sqrt{6} = 2.0$ nm, while the value of Γ translates into an interchain distance of ~4 nm, which is comparable to R_F. The self-coherence of these later results demonstrates that the Fc-PEG chains grafted at the apex of the tip form a layer of a moderate coverage of $\sim 10^{-11}$ mol/cm^2 (*i.e.*, close to the upper limit of the mushroom configuration). In other words, the tip apex is covered with a saturated layer of non-interpenetrating polymer mushrooms. This result indicates that, as previously observed for Fc-PEG layers end-grafted onto planar gold surfaces,[17,30] once a saturated PEG mushroom layer is formed, the grafted chains repel any incoming chain, hence limiting the coverage.

However, unlike what we reported previously for the case of a substrate-grafted Fc-PEG_{3400} layer, a small deviation from the above theoretical force law was observed on the experimental approach curve in the 5−10 nm region. Within this later d region, the experimental force curve was persistently observed to fall below the predicted exponential variation (see Figure 2b). This may be tentatively attributed to the sphericity of the tip, which makes the repulsive interaction between the Fc-PEG layer and the substrate less able to screen the underlying attractive gold−gold interactions that are clearly observed in the absence of the PEG layer on the tip (green dotted curve). As a result, when d is in the 6−8 nm region, the Fc-PEGylated tip is slightly attracted toward the surface, whereas for $d <$ 6 nm, the repulsive steric force arising from the compression of the chains dominates.

Current Approach Curve Analysis. Turning now to the current approach curve (Figure 2b, blue continuous line), we see that a current starts to be detected at the tip for $d \sim 12$ nm and increases continuously in intensity as d is decreased down to $d \sim 4$ nm. Upon further approach of the Fc-PEGylated tip toward the substrate, and down to $d \sim 2$ nm, the current is seen to level-off to a value of 1.9 pA. For $d < 2$ nm, the current increases rapidly as the tip is brought even closer from the underlying gold substrate. This abrupt current rise is attributed to tunneling and/or physical contact of the tip/substrate gold surfaces. As expected, when a bare tip is approached to the bare gold substrate, no current is recorded for $d >$ 1 nm (green dotted curve in Figure 2). It is also worth noting that the retraction curves, recorded when the tip was withdrawn from the substrate after hard contact, were observed to be similar to the curves recorded

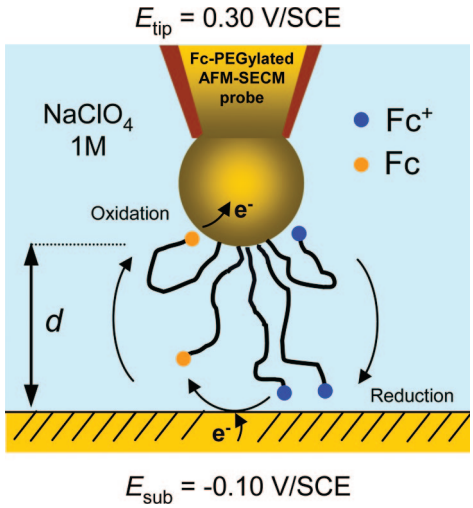

Figure 3. Working principle of Tarm/AFM-SECM microscopy. Depiction of the tip-to-substrate back and forth motion, and associated electron transfers, of the Fc heads of the PEG chains borne by the Fc-Pegylated AFM-SECM probe, giving rise to the elastic bounded diffusion SECM positive feedback current. For clarity, the tip is not drawn to scale.

during the approach, indicating that no chain loss occurred during the approach/retraction cycle and confirming the robustness of the Fc-PEG layer.

The current approach curve recorded upon approaching the Fc-PEGylated AFM-SECM probe from the bare gold substrate exhibits a strong resemblance to the one we previously reported in the case of a bare AFM-SECM probe approaching a gold substrate bearing end-grafted Fc-PEG_{3400} chains.[17,18] In order to unambiguously identify the origin of the recorded tip current, several force and current approach curves were recorded for various values of tip potential, E_{tip}. We observed that the recorded force approach curve did not depend on E_{tip} (see Supporting Information). This result confirms that the force recorded here had no electrostatic component, thanks to the high 1 M ionic strength $NaClO_4$ medium. However, the intensity of the current approach curve was observed to be a function of the tip potential. To quantify this effect, the intensity of the current plateau i_{pl}, recorded in the 2−4 nm region of the approach curves, was recorded and is plotted as a function of E_{tip} in the inset of Figure 2b. As can be seen, a characteristic i_{pl} *vs* E_{tip} S-shaped variation is obtained, which ascertains the faradic origin of the current. Moreover, the observed variation is centered around a half-wave potential of ~180 mV, which is close to the standard potential of the Fc head ($E°$ ~ 150 mV/SCE). These results unambiguously demonstrate that the tip is electrochemically contacting the Fc heads and provide strong evidence that a layer of Fc-PEG chains is indeed present at the apex of the combined probe. As represented in Figure 3, the recorded current thus results from the back and forth motion of the PEG-borne Fc heads which are alternatively oxidized at the tip and reduced at the substrate.

The occurrence of such a SECM positive feedback process[1] *validates the working principle* of the Tarm/AFM-SECM microscopy: the Fc heads of the flexible PEG chains borne by the tip are acting as *molecular nanosensors* by locally probing the electrochemical reactivity of the substrate.

As seen from the inset of Figure 2b, when the tip potential is higher than ~0.25 V/SCE, the tip plateau current, i_{pl}, no longer depends on the value of E_{tip}. Similarly, it can be shown that i_{pl} becomes E_{sub} independent for $E_{sub} < 0.05$ V/SCE. Under these conditions, the heterogeneous electron transfer steps at the tip and at the substrate are fast enough for the intensity of the feedback current to be solely conditioned by the rate of the cycling motion of the ferrocene heads, which is kinetically controlled by the flexibility of the PEG chains. Quantitative analysis of the positive feedback response can thus give access to the *dynamics* of the PEG chains. We previously modeled this feedback process for the case of substrate-bound Fc-PEG_{3400} chains contacting a large incoming spherical tip.[18] By taking into account the elastic contribution of the PEG chain to the diffusional motion of the Fc head, we were able to derive the corresponding theoretical elastic bounded diffusion feedback-current approach curve. As seen in Figure 2b (dashed curve), this theoretical approach curve can also be reasonably adjusted on the experimental data obtained for the Fc-PEGylated probe approaching a bare surface. Fitting was realized using only a single adjustable parameter, namely, $i_0 = 2\pi FDR_{tip}\Gamma/a$, a characteristic current reflecting the chain dynamics, with D the effective diffusion coefficient of the Fc heads. Using for Γ the chain coverage value determined from the analysis of the force approach curve, the best fit value of i_0 = 80 pA yields $D \sim (0.8 \pm 0.1) \times 10^{-8}$ cm^2/s. Among the five Fc-PEG tips we prepared and characterized, we found an average value for D of $(2 \pm 1) \times 10^{-8}$ cm^2/s, which is identical to the one we reported for surface-grafted Fc-PEG_{3400} chains. As discussed previously, this low D value reflects the effect of the hydrodynamics of the whole PEG chain on the motion of the Fc head.[18] In that context, the occurrence of a plateau in the current approach curve, in the d = 2−4 nm region (Figure 2b), is interpreted as resulting from compression-induced slowing of the PEG chain motion.[18] Interestingly, since the effective diffusion coefficient of the chain head is now determined, it will be possible in future work to determine the chain coverage of the probes from the *current* approach curve. Proceeding in this way is expected to be less experimentally demanding than force curve analysis since the tip spring constant and the sensitivity of the position detector of the AFM do not need to be known.

Measuring the value of the effective diffusion coefficient of the Fc head, D, is also of particular importance here since it allows one to define the rate of the fastest surface reaction that can be characterized using Tarm/

AFM-SECM with Fc-PEG-bearing probes: considering that a typical value of d for Tarm/AFM-SECM measurements is $d \sim R_F$, only surface reactions characterized by a first-order rate constant lower than $\sim D/R_F^2 = 10^5\ s^{-1}$ will be kinetically resolvable by Tarm/AFM-SECM. Surface reactions displaying faster kinetics will appear as being diffusion controlled, and the tip current will solely reflect chain dynamics. However, as a benefit of the mediator-attached configuration described here, there is no lower theoretical limit for the turnover of surface reactions, which can be kinetically characterized by Tarm/AFM-SECM. This can be demonstrated mathematically by realizing that the Tarm/AFM-SECM configuration is equivalent to a perfectly sealed thin-layer cell (TLC), whereas SECM, using a freely diffusing mediator, can be seen as a "leaky" TLC (see Supporting Information).[42] This feature makes Tarm/AFM-SECM potentially useful to characterize the functional behavior of small and slowly functioning objects such as individual enzyme molecules.

At this stage, we have demonstrated that approach curve analysis provides a unique way of fully characterizing the Fc-PEGylated probes. Not only does this analysis allow one to demonstrate specifically the presence of the Fc-PEG chains at the very tip end of the combined probe but it also allows the chain coverage, configuration, and dynamics to be determined. Most importantly, we have shown that the PEG chains are flexible enough to allow the Fc heads to efficiently electrochemically "sense" the substrate surface, a prerequisite for using the Fc-PEGylated probes for Tarm/AFM-SECM imaging. This raises the question of how many Fc-PEG molecules are actually probing the substrate surface. Beyond mere curiosity, answering this question allows the lateral electrochemical resolution of the Tarm/AFM-SECM to be predicted.

Estimating the Lateral Electrochemical Resolution of the Tarm/AFM-SECM Microscopy. Considering the fact that in the here described Tarm/AFM-SECM microscopy the surface is electrochemically "sensed" not by the AFM-SECM combined tip itself, but rather by the Fc-PEG "molecular probes", it seems legitimate to wonder about the number of Fc-PEG chains actually interacting with the substrate surface. A very coarse upper limit to that number is given by simple geometric consideration. Considering that only those chains "seeing" the substrate surface under a distance close to $d \sim R_F$ will effectively generate a feedback current, the average current carried by a single "diffusing" Fc-PEG chain would be of $\sim eD/R_F^2 \sim 13$ fA. Since for such a d value a current of 1−3 pA is typically recorded at the Fc-PEGylated probes (see Figure 2b), some 80−250 chains are involved in generating the feedback current (*i.e.*, electrochemically probing the substrate). The ability to detect such a relatively low number of chains is due to the fact that redox cycling of the Fc heads between the tip and substrate constitutes in itself an amplification mechanism that, for other systems, has been reported to even allow the detection of single molecules.[43−45]

Considering a typical chain coverage of $\Gamma \sim 1.2 \times 10^{-11}$ mol/cm^2 and a typical tip radius of ~500 nm, it can be calculated that these chains are located at the very apex of the microelectrode on a spherical cap of ~20−40 nm base radius (see Supporting Information). This result illustrates the fact that, as a direct benefit of using a mediator attached to the tip *via* nanometer-sized linear polymer chains, the interaction area between the tip and the surface represents only a small fraction of the actual size of the AFM-SECM probe. As a first approximation, this value of ~20−40 nm can be taken as an estimate of the lateral resolution of the feedback current image of Tarm/AFM-SECM microscopy attainable using the here-described Fc-PEGylated probes.

Perspectives for Tarm/AFM-SECM Imaging of a Substrate Using Fc-PEGylated Probes. Using Tarm/AFM-SEM microscopy for imaging the local electrochemical reactivity of a substrate implies being able to scan the substrate surface with the Fc-PEGylated probe, while maintaining a constant tip−substrate separation. This separation should be such that the chains can efficiently shuttle electrons to/from the tip and from/to the substrate (*i.e.*, be such that a faradic current is measured). Upon examining the current approach curve presented in Figure 2b, it can be seen that this requires $d < 12$ nm. Moreover, the requirement of recording a purely faradaic current, without any interference from tunneling or from adventitious tip−substrate contact, imposes $d > 3$ nm. To maintain a constant tip−surface distance within this range, one could consider using the tip deflection signal, resulting from the net repulsive PEG−substrate interactions observed in the force curve for $d < 6$ nm (Figure 2a), as the feedback signal in the AFM feedback loop, like classically done in force mode AFM imaging. However, one can see that this would correspond to forces ~5 nN in magnitude, which, considering a typical spring constant for our tips of ~1−3 nN/nm, and a measured sensitivity of the position sensitive detector of ~5−10 mV/nm, would translate into a 10−50 mV feedback signal. Considering that, due to the unavoidable drift of deflection signals, feedback signals as large as 1 V are classically required for comfortable imaging conditions, it seems obvious that using a force feedback mode is not appropriate for the innovative electrochemical microscopy atomic force we are developing.

Alternatively, one could also consider using a noncontact double-pass technique such as "lift mode". In this mode, each line of the image is scanned twice: once in contact to record the topography and a second time with the tip maintained at a predefined distance over the surface contour, for example, to record an electrochemical current. Indeed, "lift-mode" AFM-SECM has been successfully used to image model composite surfaces.[14] However, in this later case, a soluble mediator

was used and constant tip−substrate distances as large as ~0.2−1 μm could be maintained while still being able to record the SECM feedback current due to the freely diffusing mediator. Understandably, and as discussed above, a much shorter tip−substrate distance, in the nanometer range, would have to be maintained here, making lift mode very hard to implement for Tarm/AFM-SEM imaging. Among the other AFM "noncontact" modes, tapping mode is also of interest. In tapping mode AFM, the tip is oscillated by mechanical excitation and the tip oscillation amplitude is used as the AFM feedback signal.[46] The dependence of the oscillation amplitude on the tip−substrate separation is therefore used to maintain the tip at a constant average altitude over the substrate. Moreover, since the tip solely comes in intermittent contact with the substrate, surface lateral frictional forces are minimized, which makes this technique ideally suited for imaging fragile biological species and very attractive as a basis for the new type microscopy we propose to develop. However, using tapping mode operation for Tarm/AFM-SECM microscopy raises a fascinating question, to which we are now trying to bring an experimental answer: Can an elastic bounded diffusion feedback current be recorded at an oscillating Fc-PEGylated probe?

CONCLUSION

Combined gold AFM-SECM probes were functionalized by nanometer-sized, flexible, PEG chains bearing a ferrocene (Fc) redox label at their free end. Analysis of the force and current approach curves recorded when such Fc-Pegylated probes were approached to a bare gold substrate allowed the presence of the Fc-PEG_{3400} chains at the very tip end of the combined probes to be specifically demonstrated. It also allowed the chain coverage, configuration, and dynamics to be determined. Most importantly, we have shown that the PEG chains are flexible enough to allow their Fc heads to efficiently "sense" the substrate surface, a prerequisite for using these Fc-PEGylated probes for a decisively new type of high-resolution AFM-SECM microscopy which relies on the use of tip-attached redox-labeled polymer chains as mediators to probe the local electrochemical reactivity of a planar substrate at the nanoscale. This new type of SECM microscopy, we label Tarm (for tip-attached redox mediator)/AFM-SECM, should be particularly suitable for probing the activity of slowly functioning nanometer-sized active sites on surfaces, such as individual enzyme molecules, because it is, by design, free of the diffusional constraints which hamper the characterization of such nanosystems by classical SECM.

EXPERIMENTAL METHODS

PEG3400 Derivatives and Materials. The activated ferrocene PEG ester, Fc-PEG_{3400}-NHS (M_w = 3800, average number of OCH_2CH_2 monomer units N = 79) bearing an *N*-hydroxysuccinimide (NHS) ester at one end and a ferrocenyl (Fc) redox label at the other end, was synthesized from an analytically pure sample of Fc-PEG_{3400}-OH, free of unlabeled PEG chains, as described previously (see Supporting Information).[17,30] Matrix-assisted laser desorption/ionization time-of-flight (MALDI-TOF) mass spectra were obtained from the Université Pierre et Marie Curie, Laboratoire de Chimie Structurale Organique et Biologique (Paris, France) on a PerSeptive Biosystems Inc. (Framingham, MA) Voyager Elite instrument operating in the positive mode using 2,4,6-trihydroxyacetophenone in diammonium citrate as the matrix and 274 nm pulsed light. Cystamine (2-aminoethyl disulfide, $[NH_2\text{-}(CH_2)_2\text{-}S\text{-}]_2$) dihydrochoride and sodium perchlorate ($NaClO_4$) monohydrate were purchased from Fluka. Other commercial chemicals were reagent grade or better quality and used as received. All aqueous solutions were made with Milli-Q purified water (Millipore). All solvents used for PEG grafting of AFM-SECM probes as well as AFM-SECM experiments were filtered before use on a 0.22 μm nylon Cameo filter.

Preparation of Fc-PEG_{3400} Disulfide. A 31 mg sample of Fc-PEG_{3400}-NHS (~8.15 μmol of available NHS groups) was dissolved in 75 μL of chloroform containing triethylamine (4 μL, 18 μmol) and was treated with one-half equivalent of cystamine dihydrochloride (0.92 mg, 4.08 μmol). The reaction mixture was stirred at room temperature overnight and then passed onto a Millipore 0.45 μm Teflon membrane. After solvent removal, the resulting PEG disulfide was dissolved in methanol/ethyl acetate (50−50) and precipitated from the solution by addition of cold diethyl ether, collected by filtration, and washed copiously with ether. This workup step was repeated two times. Then drying *in vacuo* yielded Fc-PEG_{3400} disulfide (24.5 mg, M_w = 7800, 76%), which was evaluated for its identity by mass spectrometry. MALDI-TOF MS for Fc-PEG_{3400} disulfide, (+) data: m/z $(M + Na)^+$ 7789.4; the distribution of peaks (repeating units = 44 u) corresponded to average N = 79 per PEG chain, $C_{352}H_{678}O_{164}N_4S_2Fe_2Na$ requires 7789.9.

Preparation of the Template-Stripped Gold. The smooth template-stripped gold on mica substrates were prepared following a procedure adapted from the literature[47,48] and described elsewhere.[17]

Calculation of the Spring Constant of the Combined Probes. Estimation of the Spherical Microelectrode Probe Size. The spring constant of the combined probe, k_{probe}, was estimated from the measured dimensions of the flattened part of the wire-based probe that acted as a rectangular cantilever, using the formula[49] $k_{probe} = Ewt^3/4l^3$, where w, t, and l are, respectively, the cantilever width, thickness, and length and E is the elastic modulus of gold (~80 Gpa).[50] The spring constant of each probe was also measured using a reference cantilever pushing against the flexible arm of the combined AFM-SECM probe, as described in literature.[51] Both methods yielded similar spring constant values in the ~1−2 N/m range (see Supporting Information). The diameter of the spherical microelectrode tip end of the combined probes was measured by scanning electron microscopy after they were used in AFM-SECM experiments.

AFM-SECM Experiments. The AFM-SECM experiments were performed with a Molecular Imaging PICOSPM AFM microscope (Scientec, France), which was modified and operated as previously described. Experiments were carried out *in situ* in a fluid cell containing an aqueous 1 M $NaClO_4$ electrolyte solution. A homemade bipotentiostat enabled us to independently apply the electrochemical tip and substrate potentials with respect to a quasi-reference electrode (a AgCl coated silver wire). The quasi-reference electrode was separated from the working solution by a home-fabricated microseparator consisting in a capillary tube closed by a ~10 nm pore-size track-etched membrane. The counter electrode was a platinum wire. The tip and substrate currents were measured by the high (100 pA/V) and low (20 μA/V) gain current measuring circuits of the bipotentiostat. In order to make sure that no redox species were present as contaminant, in solution or on the substrate surface, voltammograms were recorded at the substrate immersed in the working solution, at

scan rate of 0.2 V/s. The voltammograms only featured capacitive background currents, with no faradaic component. During the measurements, the microscope head was placed inside a homemade vibration-proof Faraday cage. The tip-current approach curves were corrected from a small leakage current of ≤1 pA, which resulted from the imperfect insulation of the tip and of the connecting wires. This current is nonspecific and independent of the tip−substrate distance. Dozens of approach curves could be recorded with each of the ~15 Fc-PEGylated probes we successfully fabricated, demonstrating the stability of the Fc-PEG layer. In a typical experiment, the tip and substrate potentials were of $E_{tip} = +0.30$ V/SCE and $E_{sub} = -0.10$ V/SCE. A positive potential was preferentially applied to the tip in order to prevent any cathodic stripping of the Fc-PEG chains from the tip, during the time-course of the hour-long experiments. However, we verified that using $E_{tip} = -0.10$ V/SCE and $E_{sub} = +0.30$ V/SCE solely resulted in changing the sign of the recorded current and not the shape nor the intensity of the current and force approach curves. This notably indicates that the Fc heads are, in this medium, stable both in their oxidized (Fc^+) and reduced states (Fc).

Conversion of the Raw Tip Deflection Data into Force Data. The tip deflection data were acquired as a raw deflection signal from the position sensitive detector (PSD). The slope of the linear part of the contact mode approach curve, reflecting the hard contact between the tip and the substrate, was measured for each experiment and used as the characteristic sensitivity factor of the PSD. Dividing the raw deflection signal by this factor and multiplying the result by the specific spring constant of the probe, k_{probe}, then allowed the raw deflection data to be converted into force data. The tip−substrate separation was determined from the piezo elongation and tip deflection, as described previously.[17] A typical dispersion of the measured force of ±2 nN and of the tip−substrate distance of ±1 nm can be estimated from a series of approach curves recorded using a given tip (see Supporting Information).

Acknowledgment. J. Charlier from CEA/DSM-IRAMIS-SPCSI is thanked for providing the gold coated mica substrates.

Supporting Information Available: Modeling of the Tarm/AFM-SECM configuration as a thin-layer cell (TLC), derivation of the corresponding theoretical expression of the feedback current, estimation of the area of the apex of the probe occupied by the Fc-PEG chains, reproducibility of recording approach curves with a Fc-PEGylated probe, tip potential dependence of the approach curves, determination of the spring constant of the probes, synthetic route to Fc-PEG_{3400}-SS starting from analytically pure Fc-PEG_{3400}-OH, MALDI-TOF MS of Fc-PEG_{3400}-OH and Fc-PEG_{3400}-SS. This material is available free of charge *via* the Internet at http://pubs.acs.org.

REFERENCES AND NOTES

1. Bard, A. J. Introduction and Principles. In *Scanning Electrochemical Microscopy*; Bard, A. J., Mirkin, M. V., Eds.; Marcel Dekker: New York, 2001; pp 1−15.
2. Sun, P.; Laforge, F. O.; Mirkin, M. V. Scanning Electrochemical Microscopy in the 21st Century. *Phys. Chem. Chem. Phys.* **2007**, *9*, 802–823.
3. Wittstock, G.; Burchardt, M.; Pust, S. E.; Shen, Y.; Zhao, C. Scanning Electrochemical Microscopy for Direct Imaging of Reaction Rates. *Angew. Chem., Int. Ed.* **2007**, *46*, 1584–1617.
4. Borgwarth, K. and Heinze, J. Heterogeneous Electron Transfer Reactions. In *Scanning Electrochemical Microscopy*; Bard A. J., Mirkin M. V., Eds.; Marcel Dekker: New York, 2001; pp 201−238.
5. Wipf, D. O.; Bard, A. J. Scanning Electrochemical Microscopy. 10. High Resolution Imaging of Active Sites on an Electrode Surface. *J. Electrochem. Soc.* **1991**, *138*, L4–L6.
6. Engstrom, R. C.; Small, B.; Kattan, L. Observation of Microscopically Local Electron-Transfer Kinetics with Scanning Electrochemical Microscopy. *Anal. Chem.* **1992**, *64*, 241–244.
7. Lee, J.; Ye, H.; Pan, S.; Bard, A. J. Screening of Photocatalysts by Scanning Electrochemical Microscopy. *Anal. Chem.* **2008**, *80*, 7445–7450.
8. Etienne, M.; Anderson, E. C.; Evans, S. R.; Schuhmann, W.; Fritsch, I. Feedback-Independent Pt Nanoelectrodes for Shear Force-Based Constant-Distance Mode Scanning Electrochemical Microscopy. *Anal. Chem.* **2006**, *78*, 7317–7324.
9. Sun, P.; Mirkin, M. V. Kinetics of Electron-Transfer Reactions at Nanoelectrodes. *Anal. Chem.* **2006**, *78*, 6526–6534, and references cited therein. .
10. Tel-Vered, R.; Walsh, D. A.; Mehrgardi, M. A.; Bard, A. J. Carbon Nanofiber Electrodes and Controlled Nanogaps for Scanning Electrochemical Microscopy Experiments. *Anal. Chem.* **2006**, *78*, 6959–6966.
11. Watkins, J. J.; Chen, J.; White, H. S.; Abruña, H. D.; Maisonhaute, E.; Amatore, C. Zeptomole Voltammetric Detection and Electron-Transfer Rate Measurements Using Platinum Electrodes of Nanometer Dimensions. *Anal. Chem.* **2003**, *75*, 3962–3971.
12. Macpherson, J. V.; Unwin, P. R.; Hillier, A. C.; Bard, A. J. *In-situ* Imaging of Ionic Crystal Dissolution Using an Integrated Electrochemical/AFM Probe. *J. Am. Chem. Soc.* **1996**, *118*, 6445–6452.
13. Macpherson, J. V.; Unwin, P. R. Combined Scanning Electrochemical−Atomic Force Microscopy. *Anal. Chem.* **2000**, *72*, 276–285.
14. Macpherson, J. V.; Unwin, P. R. Non-Contact Electrochemical Imaging with Combined Scanning Electrochemical−Atomic Force Microscopy. *Anal. Chem.* **2001**, *73*, 550–557.
15. Kranz, C.; Friedbacher, G.; Mizaikoff, B.; Lugstein, A.; Smoliner, J.; Bertagnolli, E. Integrating an Ultramicroelectrode in an AFM Cantilever. Combined Technology for Enhanced Information. *Anal. Chem.* **2001**, *73*, 2491–2500.
16. Abbou, J.; Demaille, C.; Druet, M.; Moiroux, J. Fabrication of Submicrometer-Sized Gold Electrodes of Controlled Geometry for Scanning Electrochemical−Atomic Force Microscopy. *Anal. Chem.* **2002**, *74*, 6355–6363.
17. Abbou, A.; Anne, A.; Demaille, C. Probing the Structure and Dynamics of End-Grafted Flexible Polymer Chain Layers by Combined Atomic Force−Electrochemical Microscopy. Cyclic Voltammetry within Nanometer-Thick Macromolecular Poly(ethylene glycol) Layers. *J. Am. Chem. Soc.* **2004**, *126*, 10095–10108.
18. Abbou, J.; Anne, A.; Demaille, C. Accessing the Dynamics of End-Grafted Flexible Polymer Chains by Atomic Force-Electrochemical Microscopy. Theoretical Modeling of the Approach Curves by the Elastic Bounded Diffusion Model and Monte Carlo Simulations. Evidence for Compression-Induced Lateral Chain Escape. *J. Phys. Chem. B* **2006**, *110*, 22664–22675.
19. Frederix, P. L. T. M.; Gullo, M. R.; Akiyama, T.; Tonin, A.; de Rooij, N. F.; Staufer, U.; Engel, A. Assessment of Insulated Conductive Cantilevers for Biology and Electrochemistry. *Nanotechnology* **2005**, *16*, 997–1005.
20. Gullo, M. R.; Frederix, P. L. T. M.; Akiyama, T.; Engel, A.; de Rooij, N. F.; Staufer, U. Characterization of Microfabricated Probes for Combined Atomic Force and High-Resolution Scanning Electrochemical Microscopy. *Anal. Chem.* **2006**, *78*, 5436–5442.
21. Hirata, Y.; Yabuki, S.; Mizutani, F. Application of Integrated SECM Ultra-Micro-Electrode and AFM Force Probe to Biosensor Surfaces. *Bioelectrochem.* **2004**, *63*, 217–224.
22. Fasching, R. J.; Tao, Y.; Prinz, F. B. Cantilever Tip Probe Arrays for Simultaneous SECM and AFM Analysis. *Sens. Actuators, B* **2005**, *108*, 964–972.
23. Wipf, D. O.; Bard, A. J. Scanning Electrochemical Microscopy. Part 7. Effect of Heterogeneous Electron-Transfer Rate at the Substrate on the Tip Feedback Current. *J. Electrochem. Soc.* **1991**, *138*, 469–474.
24. Bard, A. J.; Mirkin, M. V.; Unwin, P. R.; Wipf, D. O. Scanning Electrochemical Microscopy. 12. Theory and Experiment of the Feedback Mode with Finite Heterogeneous Electron-

Transfer Kinetics and Arbitrary Substrate Size. *J. Phys. Chem.* **1992**, *96*, 1861–1868.
25. Pierce, D. T.; Unwin, P. R.; Bard, A. J. Scanning Electrochemical Microscopy. 17. Studies of Enzyme-Mediator Kinetics for Membrane- and Surface-Immobilized Glucose Oxidase. *Anal. Chem.* **1992**, *64*, 1795–18004.
26. Pierce, D. T.; Bard, A. J. Scanning Electrochemical Microscopy. 23. Retention Localization of Artificially Patterned and Tissue-Bound Enzymes. *Anal. Chem.* **1993**, *65*, 3598–3604.
27. Johnson, K. A. In *The Enzymes*; Sigman, D. S., Ed.; Academic Press: San Diego, CA, 1992; Vol. 20, pp 1−60.
28. Hudson, J. E.; Abruña, H. D. Electrochemically Controlled Adhesion in Atomic Force Spectroscopy. *J. Am. Chem. Soc.* **1996**, *118*, 6303–6304.
29. Diaz, D. J.; Hudson, J. E.; Storrier, G. D.; Abruña, H. D.; Sundararajan, N.; Ober, C. K. Lithographic Applications of Redox Probe Microscopy. *Langmuir* **2001**, *17*, 5932–5938.
30. Anne, A.; Moiroux, J. Quantitative Characterization of the Flexibility of Poly(ethylene glycol) Chains Attached to a Glassy Carbon Electrode. *Macromolecules* **1999**, *32*, 5829–5835.
31. Anne, A.; Demaille, C.; Moiroux, J. Terminal Attachment of Polyethylene Glycol (PEG) Chains to a Gold Electrode Surface. Cyclic Voltammetry Applied to the Quantitative Characterization of the Flexibility of the Attached PEG Chains and of Their Penetration by Mobile PEG Chains. *Macromolecules* **2002**, *35*, 5578–5586.
32. Anicet, N.; Anne, A.; Bourdillon, C.; Demaille, C.; Moiroux, J.; Savéant, J.-M. Electrochemical Approach to the Dynamics of Molecular Recognition of Redox Enzyme Sites by Artificial Cosubstrates in Solution and in Integrated Systems. *Faraday Discuss.* **2000**, *116*, 269–279.
33. Anne, A.; Demaille, C; Moiroux, J. Elastic Bounded Diffusion and Electron Propagation. Dynamics of the Wiring of a Self-Assembly of Immunoglobulins Bearing Terminally Attached Ferrocene Poly(ethylene glycol) Chains According to a Spatially Controlled Organization. *J. Am. Chem. Soc.* **2001**, *123*, 4817–4825.
34. Grosberg, A. Y.; Khokhlov, A. R. *Statistical Physics of Macromolecules*; American Institute of Physics: New York, 1994; pp 1−144.
35. de Gennes, P. G. *Scaling Concepts in Polymer Physics*; Cornell University Press: Ithaca, NY, 1991; pp 29−53.
36. Kenworthy, A. K.; Hristova, K.; Needham, D.; McIntosh, T. J. Range and Magnitude of the Steric Pressure Between Bilayers Containing Phospholipids with Covalently Attached Poly(ethylene glycol). *Biophys. J.* **1995**, *68*, 1921–1936.
37. Hansen, P. L.; Cohen, J. A.; Podgornik, R.; Parsegian, V. A. Osmotic Properties of Poly(Ethylene Glycols): Quantitative Features of Brush and Bulk Scaling Laws. *Biophys. J.* **2003**, *84*, 350–355.
38. Gabriel, S.; Jerôme, C.; Jerôme, R.; Fustin, C.-A.; Pallandre, A.; Plain, J.; Jonas, A. M.; Duwez, A.-S. One-Step Polymer Grafting from Silicon Nitride SPM Probes: From Isolated Chains to Brush Regime. *J. Am. Chem. Soc.* **2007**, *129*, 8410–8411.
39. Israelachvili, J. *Intermolecular and Surface Forces*, 2nd ed.; Academic Press: San Diego, CA, 1992; pp 288−311.
40. Dolan, A. K.; Edwards, S. F. Theory of the Stabilization of Colloids by Adsorbed Polymer. *Proc. R. Soc. London, Ser. A* **1974**, *337*, 509–516.
41. Garnier, L.; Gauthier-Manuel, B.; van der Vegte, E. W.; Snijders, J.; Hadziioannou, G. Covalent Bond Force Profile and Cleavage in a Single Polymer Chain. *J. Chem. Phys.* **2000**, *113*, 2497–2503.
42. Bard, A. J.; Denuault, G.; Chongmok, L.; Mandler, D.; Wipf, D. O. Scanning Electrochemical Microscopy: A New Technique for the Characterization and Modification of Surfaces. *Acc. Chem. Res.* **1990**, *23*, 357–363.
43. Fan, F.-R. F.; Bard, A. J. Electrochemical Detection of Single Molecules. *Science* **1995**, *267*, 871–874.
44. Fan, F.-R. F.; Juhyoun Kwak, J.; Bard, A. J. Single Molecule Electrochemistry. *J. Am. Chem. Soc.* **1996**, *118*, 9669–9675.
45. Sun, P.; Mirkin, M. V. Electrochemistry of Individual Molecules in Zeptoliter Volumes. *J. Am. Chem. Soc.* **2008**, *130*, 8241–8250.
46. *Applied Scanning Probe Methods*, Bhushan, B., Fuchs, H., Hosaka, S., Eds.; Springer-Verlag: Berlin, 2004; pp 230−254.
47. Hegner, M.; Wagner, P.; Semenza, G. Ultralarge Atomically Flat Template-Stripped Au Surfaces for Scanning Probe Microscopy. *Surf. Sci.* **1993**, *291*, 39–46.
48. Wagner, P.; Hegner, M.; Güntherodt, H.-J.; Semenza, G. Formation and *In Situ* Modification of Monolayers Chemisorbed on Ultraflat Template-Stripped Gold Surfaces. *Langmuir* **1995**, *11*, 3867–3875.
49. Sader, J. E.; Chon, J. W. M.; Mulvaney, P. Calibration of Rectangular Atomic Force Microscope Cantilevers. *Rev. Sci. Instrum.* **1999**, *70*, 3967–3969.
50. Sader, J. E.; Larson, I.; Mulvaney, P.; White, L. R. Method for the Calibration of Atomic Force Microscope Cantilevers. *Rev. Sci. Instrum.* **1995**, *66*, 3789–3798.
51. Gates, R. S.; Reitsma, M. G. Precise Atomic Force Microscope Cantilever Spring Constant Calibration Using a Reference Cantilever Array. *Rev. Sci. Instrum.* **2007**, *78*, 0861011–0861013.